Journal of Molecular Histology (2025) 56:74
https://doi.org/10.1007/s10735-024-10350-x

ORIGINAL PAPER

A determination of the main regulators of necroptosis in testicular tissue under different heat stresses

Musa Tatar[1] · **Kıymet Kübra Tüfekci**[2] · **Sema Uslu**[3]

Received: 8 November 2024 / Accepted: 29 December 2024 / Published online: 25 January 2025

Abstract

Although minimal increases in testicular temperature can compromise spermatogenesis and lead to fertility-related problems, the basic mechanism involved in germ cell destruction as a response to heat stress is still unclear. However, necroptosis is known to regulate a number of physiological and pathological events. This study investigated the role of RIPK1/RIPK3 and MLKL, the main regulators of necroptosis, against different heat stresses in testis tissue. Forty-two *Wistar albino* rats were divided into seven groups: six experimental exposed to heat stress and one control. Heat stress was induced by causing the rats to swim for 30 min daily for 60 days in a water bath at temperatures of 39 °C and 43 °C. Testis tissues were collected while the animals were under anesthesia on the 1st, 7th, and 14th days after 60 days of heat application. The tissues were first fixed in Bouin's solution. After routine histological procedures, immunohistochemical staining was performed on one-half of the tissues using RIPK1/RIPK3 and MLKL primary antibodies on serially collected 5 µm-thick sections. Immunoblotting analysis was performed on the other half. Analyses revealed an increase in the expression of RIPK1/RIPK3 and MLKL proteins, regulators of necroptosis, in both the 39 °C and 43 °C groups, although this was greater in the tissue exposed to 43 °C heat stress. These molecules were also especially affected by round and elongated spermatids, and reactivity was observed in Leydig cells. In conclusion, exposure to increased temperature may cause RIPK1/RIPK3 and MLKL-mediated cellular changes in the testis.

Keywords Heat stress · Testis · Necroptosis · Infertility

Introduction

Due to the climate change caused by worldwide record temperatures in recent years, the number of heat-related diseases is expected to continue to increase. Despite research into the mechanisms underlying the effects of heat stress on tissues, mortality rates, and tissue dysfunctions due to heat stress continue to rise (Pryor et al. 2015; Gu et al. 2016; Wang et al. 2016; Li et al. 2020). A comprehensive investigation of the conditions that cause male infertility is needed to halt or prevent factor-induced infertility and to determine new treatment procedures.

High temperature is associated with heat stress, a phenomenon capable of causing molecular and physiological changes in and affecting the functions of mammalian reproductive organs. Heat stress also affects reproductive characteristics due to global warming (Hansen 2009; Boni 2019; Morrell 2020; Ngoula et al. 2020). The significance of thermoregulation lies in that even very small temperature rises can compromise spermatogenesis and fertility problems. In

✉ Musa Tatar
musatatar88@hotmail.com; mtatar@kastamonu.edu.tr

Kıymet Kübra Tüfekci
kubrayurt55@gmail.com

Sema Uslu
semauslu43@hotmail.com

[1] Department of Histology and Embryology, Faculty of Veterinary Medicine, Kastamonu University, Kastamonu, Türkiye

[2] Department of Histology and Embryology, Faculty of Medicine, Kastamonu University, Kastamonu, Türkiye

[3] Department of Histology and Embryology, Faculty of Veterinary Medicine, Sivas Cumhuriyet University, Sivas, Türkiye

pathological conditions such as heat stress, various mechanisms develop in testis tissues that are triggered by exposure to stress, including DNA repair, heat shock response, oxidative stress response, apoptosis, and cell death (Paul et al. 2009). Increased testicular temperatures cause germ cell damage, adversely affecting spermatogenesis and fertility (Shakeel and Yoon 2023). Temperature changes in the testicular tissue also lead to germinal epithelial atrophy and spermatogenic retention, decreasing sperm count. Sertoli and Leydig cells are also affected by heat stress. Atrophy of the testes and impairment of spermatogenesis due to heat stress are among the causes of male infertility (Skandhan and Rajahariprasad 2007; Hughes and Acerini 2008).

Necroptosis is a form of programmed cell death that exhibits the morphological characteristics of necrosis that occur during biological processes, such as inflammation, immune response, embryonic development, and metabolic abnormalities. It is currently regarded as crucial in regulating various physiological processes. Despite much research into necroptosis, many uncertainties persist concerning its mechanisms, triggers, and physiological roles (Meng et al. 2016). Studies have reported that experiments into cell death pathways and the treatment of diseases through these lack definitive evidence supporting the important role of necroptosis in the pathology of diseases (Wallach et al. 2016; Weinlich et al. 2017). RIPK1, RIPK3, and MLKL are critical regulators of necroptosis, a highly pro-inflammatory form of cell death implicated in various pathological processes and diseases (Xu et al. 2019). RIPK3 knockout mice exhibit less tissue injury in various chemical or ischemic reperfusion-induced tissue damage models. Necroptosis is, therefore, thought to play significant roles under conditions of pathological tissue damage. However, no marked developmental, physiological, or fertility problems have been reported in RIPK3 or MLKL knockout mice. The role of the main regulators of necroptosis in pathological conditions in testicular tissue is also not fully understood. The principal subject of investigation in this research field is which tissue necroptosis occurs in, and under what physiological conditions (Robinson et al. 2012; Murphy et al. 2013; Wu et al. 2013; Xu et al. 2019). Studies have reported that both RIPK3- and MLKL-knockout mice maintain the 'youthful' morphology of the male reproductive organs and function at an advanced age. In contrast, their occurrence in wild-phenotype mice of the same age disrupts genital organ physiology. These knockout mice exhibiting excellent fertility even at advanced ages revealed that necroptosis plays a role in promoting the aging of the male mouse reproductive system. Necroptosis has been observed in spermatogonial stem cells in the testes of old mice and has been described as encouraging aging-related impairment of the male reproductive system (Li et al. 2017; Xie et al. 2020).

Whether necroptosis, found to exist under physiological and pathological conditions in many studies, is involved in heat stress in testis tissue in rats is still unknown. The purpose of this study was therefore, to examine the role of the main regulators of necroptosis on the 1st, 7th, and 14th days after heat stress induced during spermatogenesis in testis tissues at different temperatures (39 °C and 43 °C) using both immunohistochemical and immunoblotting methods.

In our study, the selection of 39 °C and 43 °C aimed to investigate how necroptosis mechanisms are triggered at the physiological upper limit of testicular temperature (39 °C) and under extreme stress conditions (43 °C). As 39 °C is close to the physiological temperature threshold for the testis, it may allow the identification of the initiation of cellular adaptation or damage mechanisms, such as necroptosis.

In the literature, 43 °C has been shown to induce cellular stress responses, including oxidative stress, DNA damage, and apoptosis. Understanding how exposure to this temperature affects proteomic changes or the expression levels of specific proteins may elucidate their adaptive or protective roles (Kumar Roy et al. 2016; Hasani et al. 2020).

Materials and methods

The study was conducted with the permission of the Kastamonu University Experimental Animal Ethics Committee (date 24.06.2022, number 11). In this study, 42 male Wistar albino rats, 90 days old (220–240 gr) were used. The animals received standard pellet feed in a 12-hour light/12-hours dark cycle. Seven groups of six animals each were constituted and exposed to heat stress for 60 days. During the application, the inguinal area was floated in hot water for 30 min at temperatures of 39 °C and 43 °C, these being frequently checked by means of a thermometer. No procedure was performed on the control group animals. At the end of the 60-day application, tissues were collected from the 39 °C and 43 °C groups following sacrifice by decapitation on the 1st, 7th, and 14th days. The left testis from each animal was fixed with Bouin's solution for 24 h for routine tissue tracking procedures. The tissue tracking process commenced with passage through a graded alcohol series. Histopathological analyses and immunohistochemical staining were performed on 5-micron sections taken from tissue blocks. Right testicular tissue was stored at −80 °C for protein extraction for Western blot analysis. Histological examination was performed in the Kastamonu University Faculty of Medicine Department of Histology and Embryology research laboratory, and Western blotting analysis in the Kastamonu University Faculty of Veterinary Medicine Department of Histology and Embryology research laboratory.

Histopathological analysis and Johnsen score

Sections taken for histopathological analysis and Johnsen score were stained with hematoxylin and eosin. The Johnsen score was calculated to evaluate the spermatogenesis status and cellular organization of the seminiferous tubules in testicular sections. This score has a value between 1 and 10 according to the degree of spermatogenesis in the tubules. For this purpose, at least 40–50 seminiferous tubules were examined per section and each section was scored histopathologically using the Johnson score. Seminiferous tubules were scored on a scale of 1 to 10 according to the Johnsen criteria; 1: no cells; 2: Sertoli cells without germ cells; 3: only spermatogonia; 4: only a few spermatocytes; 5: no spermatozoa or spermatids but many spermatocytes; 6: only a few spermatids; 7: no spermatozoa but many spermatids; 8: only a few spermatozoa; 9: many spermatozoa but irregular spermatogenesis; 10: complete spermatogenesis and perfect tubules (Johnsen 1970).

Immunohistochemical analysis

Serial sections 5-µm in thickness from the prepared paraffin blocks were placed onto adhesive slides. The streptavidin-biotin complex (sABC) staining method was then applied to determine RIPK1, RIPK3, and MLKL reactivity in the sections. Antigen retrieval was performed once the sections had been deparaffinized in xylol and dehydrated by passage through alcohol series. For that purpose, the slides were placed into a 10-fold diluted citrate buffer (citrate buffer heat-induced epitope retrieval pH: 6) solution and heated in a microwave oven at 800 Watts for 20 min. Following this process, the sections were left to cool for 30 min. After washing in phosphate buffered saline (PBS) solution for 3 × 5 min, they were next incubated in 3% hydrogen peroxide (hydrogen peroxide 30% Merck: 108597) solution in the dark for 20 min for the purpose of blocking endogenous peroxidase activity. At the end of the incubation procedure, the sections were rewashed with PBS solution for 3 × 5 min. In order to prevent nonspecific antibody binding, Ultra V Block (TP-125-HL, Thermo Fisher Scientific) solution was dropped onto the tissues, left for 10 min. Then, they were incubated at +4 °C overnight at appropriate concentrations of primary antibodies without washing (Table 1). Following incubation, the sections were washed with PBS for 3 × 5 min. Secondary antibody kits (TP-125-HL, Thermo Fisher Scientific) were then applied in line with the procedure order and duration, after which AEC chromogen (TA-060-HA, Thermo Fisher Scientific) was applied to show the reaction and render the immunoreactivity visible. A water-compatible covering medium (TA-125-UG, Thermo Fisher Scientific:) was applied to the sections counterstained with Gill's hematoxylin were and examined under a microscope. In the negative controls, PBS replaced the primary antibody after protein blocking, and the tissues were incubated with that solution overnight.

Table 1 Primary antibodies used in immunohistochemical staining and immunoblotting

	Dilution			
Primary antibody	**IHC**	**WB**	**Code**	**Company**
RIPK1-Specific polyclonal antibody	1:100	1:1000	17519-1-AP	Proteintech
RIPK3-Specific polyclonal antibody	1:100	1:500	17563-1-AP	Proteintech
MLKL- Monoclonal antibody	1:500	1:3000	66675-1-Ig	Proteintech

Western blot analysis

Testis tissues collected at the conclusion of the experiment were homogenized using RIPA lysis buffer (sc-24948/SantaCruz) containing a protease inhibitor mixture. Total cellular protein concentrations were calculated by means of a Bicinchoninic Acid kit (SMART™ BCA Protein Assay Kit/21071 iNtRON Biotechnology). Briefly, the protein specimens were first boiled with sample buffer for 10 min at 95 °C. Next, 20 µg of total protein sample was loaded onto 10% polyacrylamide gel and exposed to electrophoresis in a running buffer solution at 150 V for 1 h (Kurien and Scofield 2015). The separated proteins were then transferred from SDS-PAGE to the PVDF membrane. They were next blocked for 1 h in 5% skimmed milk powder at room temperature and incubated overnight together with the primary antibodies presented in Table 1 at 4 °C. The membranes were next washed with Tris buffer for 15 min and exposed to horseradish peroxidase-conjugated secondary antibodies (1/10000) for a further 1 h at room temperature. Following this secondary treatment, the membranes were washed in triplicate using PBS-T for 5 min. The protein signals were detected with BioRad (Clarity Western ECL Substrate, 1705060) using Image Studio™ Lite (LICOR). ImageJ software (Image Analysis Software; Image J version 1.52, National Institutes of Health, USA) was employed to measure the area of the sample protein bands on the membrane. When determining the band intensity of the proteins under examination, normalization was calculated as arbitrary units, defined as the ratio of these proteins to the β-actin proteins employed as the endogenous control (Jiang et al. 2023).

Statistical analysis

Normality and homogeneity of variances were verified to meet the assumptions of parametric tests before commencement of the data analysis. The study data were evaluated with the Mann-Whitney test or one-way analysis of variance (ANOVA), while the Duncan test was used to determine intergroup differences. The study data were expressed as mean ± standard deviation (SD). SPSS version 22.0 for Windows software (IBM, New York, ASA) was used for all analyses, and $p < 0.05$ was considered significant.

Results

Histopathological analysis and Johnsen score results

It was observed that the histological architecture of the testicular tissue in the control group was regular, and the seminiferous tubules were clearly and regularly located. The spermatozoa density in the tubule lumen was normal. Sertoli cells and the germinal epithelial layer appeared intact and healthy. Leydig cells were distributed homogeneously in the interstitial tissue, and no inflammation, necrosis or fibrosis was observed. It was determined that the images of the testicular sections of the 39 °C 1st day group were similar to the control. Vacuolization and sub-basal vacuolization were observed in the seminiferous tubules of the 39 °C 7th and 14th groups. Tubular atrophy and vacuoles were seen in all 43 °C groups. In addition, shedding of the germ cell line was detected on the 14th day of 43 °C (Fig. 1).

Based on the statistical evaluation of Johnsen scores, the Control group exhibited the highest score, indicating that the testicular tissue preserved its normal histological structure. In the 39 °C group, no statistically significant differences were observed in Johnsen scores on the 1st and 7th days compared to the Control group ($p > 0.05$). However, a significant decrease was noted on the 14th day, with a statistically significant difference compared to the Control group ($p < 0.001$). In the 43 °C group, the Johnsen score on the 1st day showed a statistically significant reduction compared to the Control group ($p < 0.001$). This decline became more pronounced on the 7th day, accompanied by severe disruptions in the histological structure of the testicular tissue ($p < 0.001$). By the 14th day, the 43 °C group exhibited the lowest Johnsen score, indicating extensive histological damage to the testicular tissue ($p < 0.001$), (Fig. 1).

Immunohistochemical results

Analysis revealed weak positive RIPK1 immunoreactivity in testis sections from control group spermatids and moderate RIPK1 immunoreactivity in Leydig cells (Fig. 2). Among the groups subjected to 39 °C heat stress, RIPK1 immunoreactivity was weak in Leydig cells on the 1st day. On the 7th days, moderate immunoreactivity was detected Leydig cells, and weak immunoreactivity in the muscular layer of blood vessels. On day 14, moderate RIPK1 immunoreactivity was detected in Leydig cells, and weak immunoreactivity in the muscular layer of blood vessels. RIPK1 immunoreactivity was evident in step 12 and step 14 elongated spermatids at stages XII and XIV in all 39 °C heat stress groups. Additionally, mature (step19) spermatids at stage VII-VIII were immunoreactive positive (Fig. 3; Table 2).

In the groups subjected to 43 °C heat stress, RIPK1 immunoreactivity on the 1st day was weak in the spermatogonia and the muscular layer of blood vessels and moderate in spermatid and Leydig cells. On the 7th day, RIPK1 immunoreactivity was weak in spermatogonia and Leydig cells and moderate in spermatids, while on the 14th day, moderate RIPK1 immunoreactivity was detected in spermatogonia and Leydig cells. In all 43 °C heat stress RIPK1 immunoreactivity was found in stage XII and XIV, step 12 and step 14 elongating spermatids, and stage VII-VIII mature (step 19) spermatids (Fig. 3; Table 2).

Weak RIPK3 immunoreactivity was detected in the control group spermatids, Leydig cells, and the muscular layer of blood vessels (Fig. 2).

RIPK3 immunoreactivity was observed in varying degrees in the experimental groups, except for the 43 °C 14th day group, with the majority of immunoreactivity in stage XII and stage XIV pachytene and diplotene spermatocytes, while positivity was observed in a small number of stage VII and stage VII round spermatids. Positivity was detected in the interstitial area in the 43 °C 14th day group.

In the groups exposed to 39 °C heat stress, weak immunoreactivity was detected in the spermatocyte on the 1st day, moderate RIPK3 immunoreactivity in spermatocyte on the 7th day and 14th day, and no staining in other cells. On the 14th day, RIPK3 staining was negative in spermatogonia and spermatid cells (Fig. 4; Table 3).

Moderate positive RIPK3 staining was observed in spermatocytes and negative staining in Leydig cells on the 1st day in the 43 °C heat stress groups. On the 7th day, RIPK3 immunoreactivity was moderate in spermatocytes and negative in Leydig cells. On the 14th day, RIPK3 immunoreactivity was weak in spermatogonia and Leydig cells (Fig. 4; Table 3).

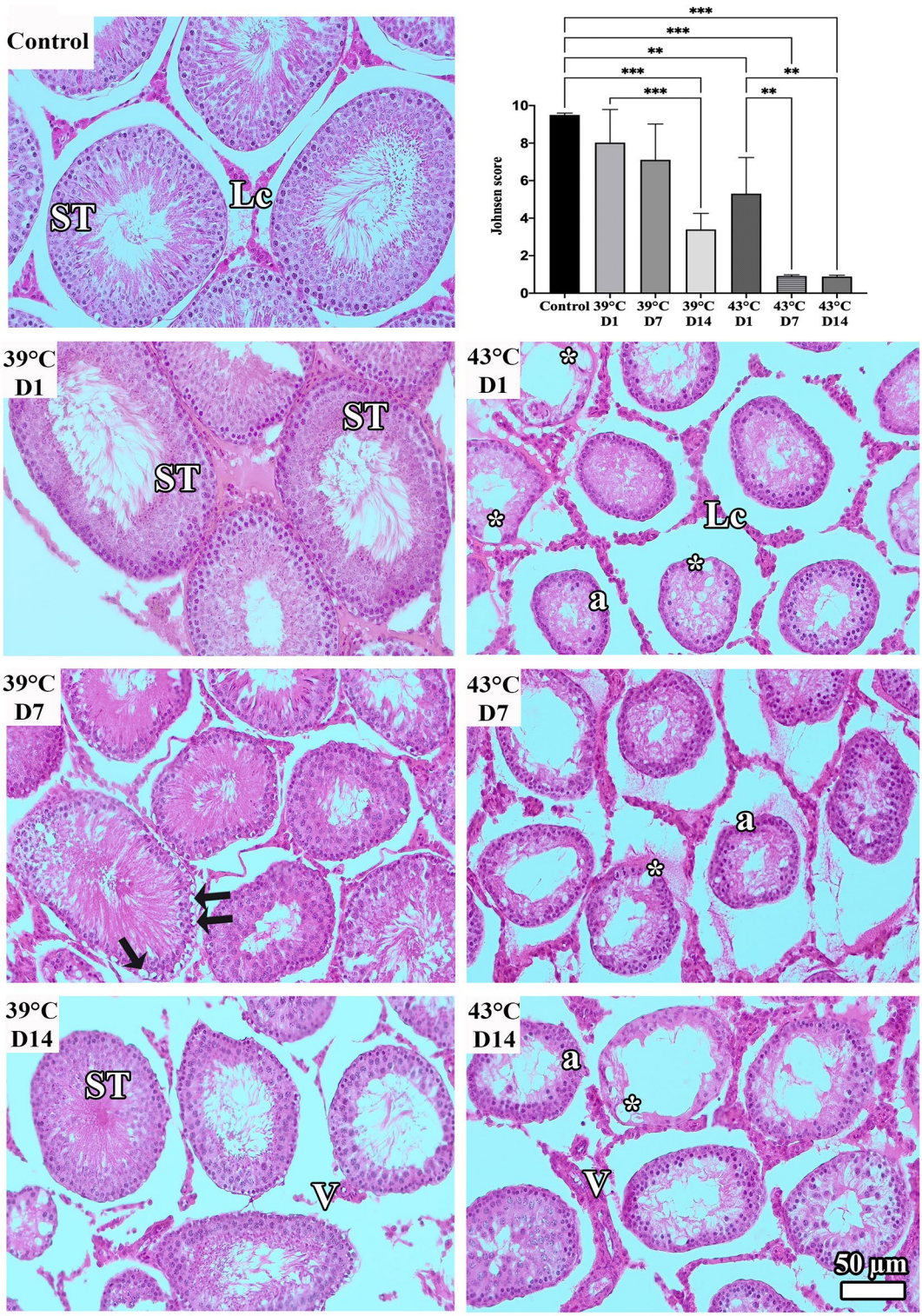

Fig. 1 Hematoxylin eosin staining of testis sections and Johnsen score analysis from all groups. Lc; Leydig cell, ST; seminiferous tubule, star; vacuolization, black arrow; sub-basal vacuolization, a; tubular atrophy, V; vessel. Scale bar 50 µm for all panels. (*$p<0.05$, **$p<0.01$, ***$p<0.001$)

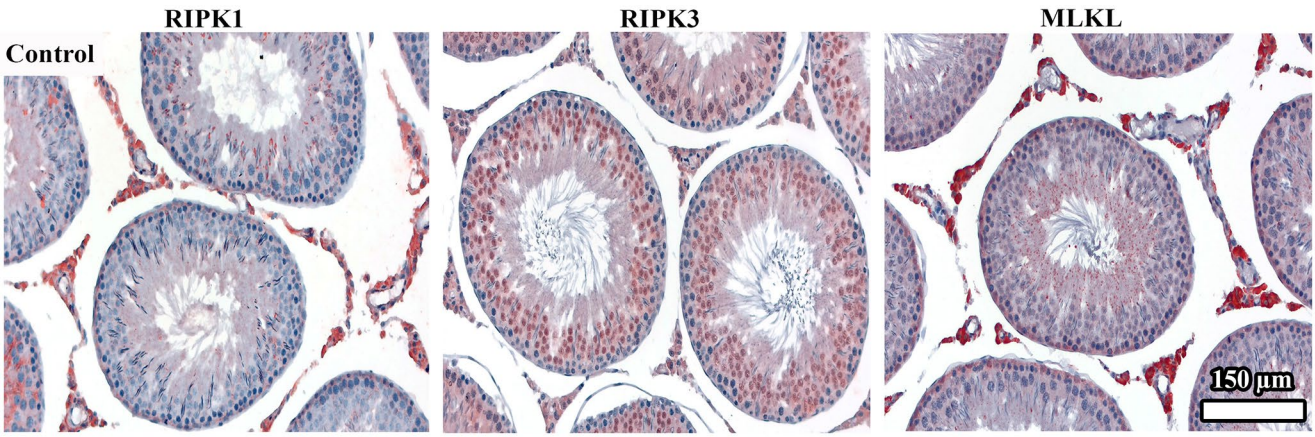

Fig. 2 Anti-RIPK1, anti-RIPK3 and anti-MLKL immunohistochemical staining of testis sections from control groups. Scale bar show 150 µm

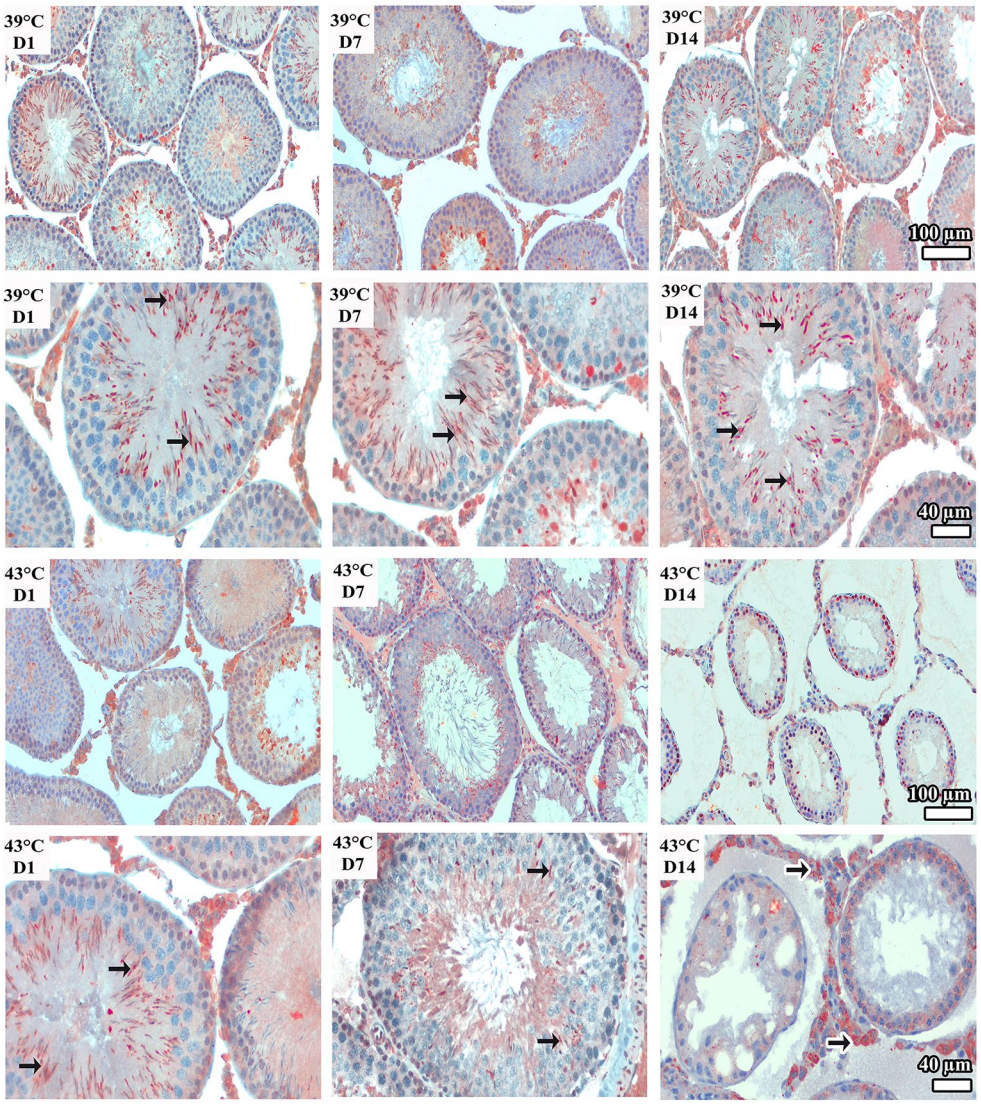

Fig. 3 Anti-RIPK1 immunohistochemical staining of testis sections from all groups. Black arrow; stage XII and XIV (step 12/14) elongating spermatids, stage VII-VIII mature (step 19) spermatids, white framed arrow; interstitial area immune reactivity. Counterstaining was performed with Gill's hematoxylin. Scale bars show 100 µm and 40 µm

Table 2 Semiquantitative analyses of the immunohistochemical staining of RIPK1 in testis tissue. (0: negative; +: weak positive; ++: moderate positive; +++: strong positive staining)

anti-RIPK1 immunostaining							
Cell type	Control	39 °C D1	39 °C D7	39 °C D14	43 °C D1	43 °C D7	43 °C D14
Spermatogonium	0	0	0	0	+	+	++
Spermatocyte	0	0	0	0	0	0	0
Spermatid	+	++	++	++	++	++	0
Leydig cells	++	+	++	++	++	+	++
Peritubular myoid cells	0	0	0	0	0	0	0
Vessel wall muscles	0	0	+	+	+	0	0

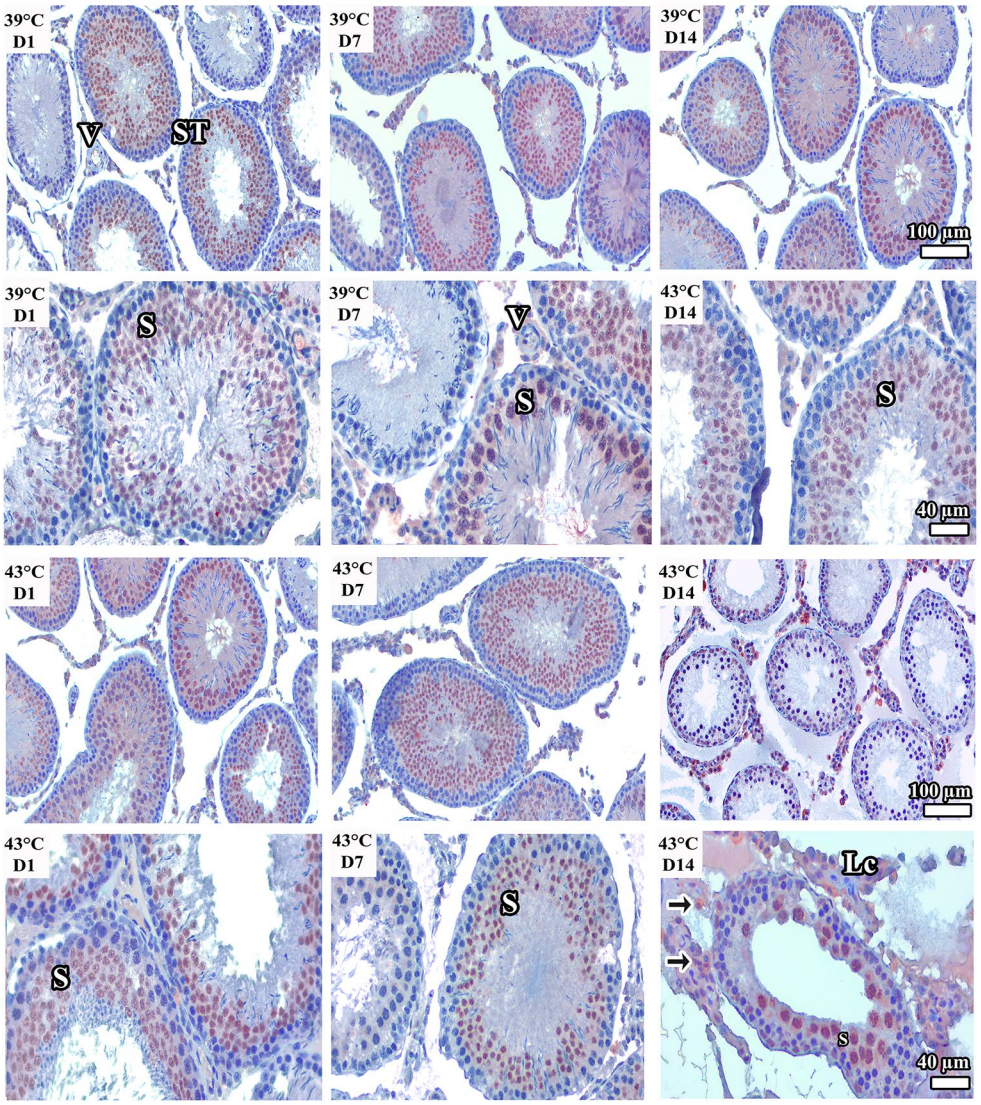

Fig. 4 Anti-RIPK3 immunohistochemical staining of testis sections from all groups. Lc; Leydig cell, ST; seminiferous tubule, S; stage 12 and 14 pachytene and diplotene spermatocytes, V; vessel, white framed arrow; interstitial area immune reactivity. Counterstaining was performed with Gill's hematoxylin. Scale bars show 100 µm and 40 µm

Evaluation of MLKL immunoreactivity revealed that the control group spermatids were weakly stained, and the Leydig cells were moderately positively stained (Fig. 2). MLKL immunoreactivity was detected in stage VII-VIII and stage XII-XIV spermatogonia and Leydig cells on the 1st and 7th days in the 39 °C heat stressed groups, and moderate positive immunoreactivity was observed only in Leydig cells on the 14th day (Fig. 5; Table 4).

Moderate MLKL immunoreactivity was detected on the 1st day in the Leydig cells of the groups subjected to 43 °C heat stress. On the 7th day, weak immunoreactivity was detected in spermatogonia and the muscular layer of blood vessels, and moderate immunoreactivity was detected in

Table 3 Semiquantitative analyses of the immunohistochemical staining of RIPK3 in testis tissue. (0: negative; +: weak positive; ++: moderate positive; +++: strong positive staining)

anti-RIPK3 immunostaining							
Cell type	Control	39 °C D1	39 °C D7	39 °C D14	43 °C D1	43 °C D7	43 °C D14
Spermatogonium	0	0	0	0	0	0	+
Spermatocyte	0	+	++	++	++	++	0
Spermatid	0	0	0	0	0	0	0
Leydig cells	+	0	0	0	0	0	+
Peritubular myoid cells	0	0	0	0	0	0	0
Vessel wall muscles	+	0	0	0	0	0	0

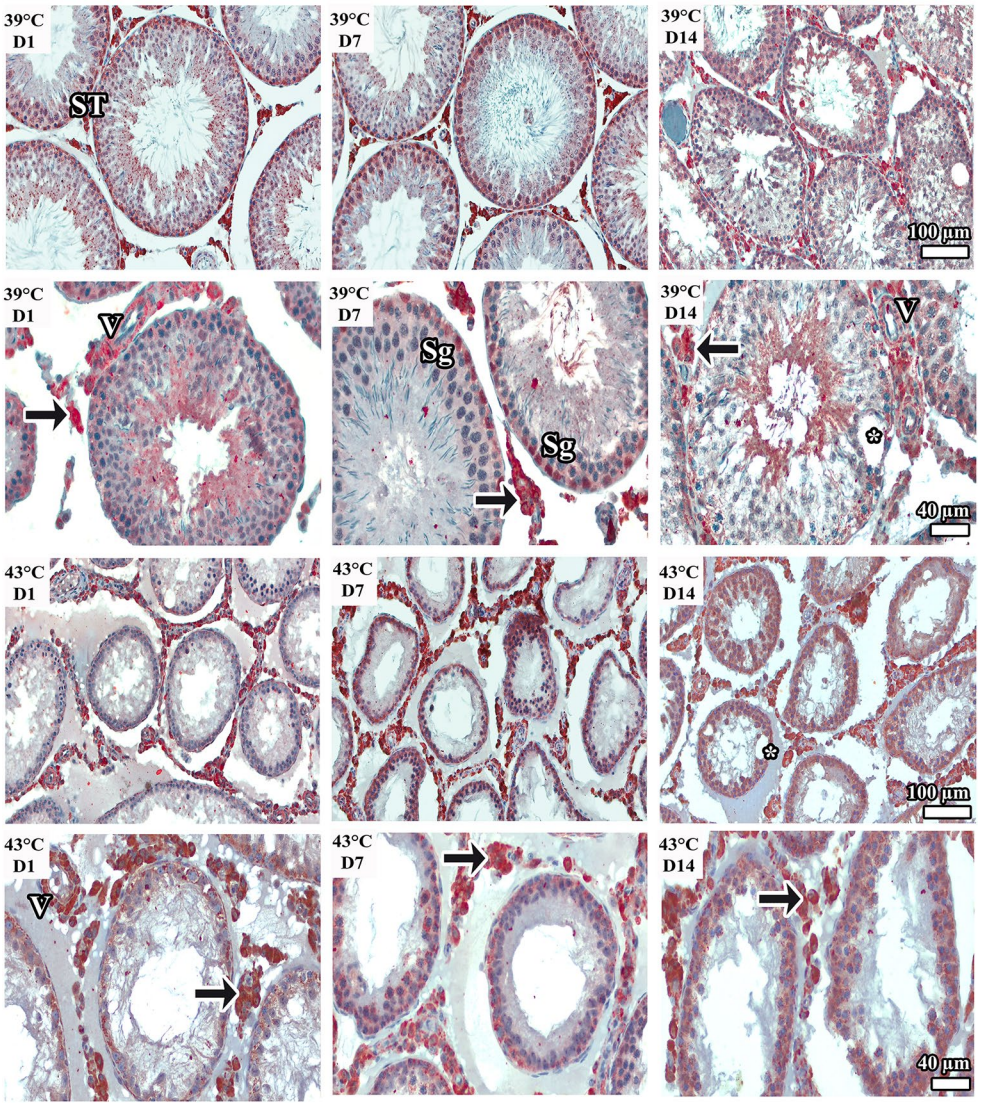

Fig. 5 Anti-MLKL immunohistochemical staining of testicular sections of all groups. ST; seminiferous tubule, Sg; spermatogonium, V; vessel, star; vacuolization, white framed arrow; interstitial area immune reactivity. Counterstaining was performed with Gill's hematoxylin. Scale bars show 100 µm and 40 µm

Leydig cells. On the 14th day, weak MLKL immunoreactivity was detected in the muscular layer of blood vessels and spermatogonia, and peritubular myoid cells, and moderate immunoreactivity in Leydig cells (Fig. 5; Table 4).

Western blot findings

A comparison of the levels of RIPK1, RIPK3 and MLKL proteins obtained by immunoblotting method revealed a statistically significantly higher RIPK1 protein level than in the control group on the 1st day of 39 °C heat stress ($p<0.05$). However, no differences compared to the control

Table 4 Semiquantitative analyses of the immunohistochemical staining of MLKL in testis tissue. (0: negative; +: weak positive; ++: moderate positive; +++: strong positive staining)

Cell type	Control	39 °C D1	39 °C D7	39 °C D14	43 °C D1	43 °C D7	43 °C D14
Spermatogonium	0	++	++	0	0	+	+
Spermatocyte	0	0	0	0	0	0	+
Spermatid	+	+	+	0	0	0	0
Leydig cells	++	++	++	++	++	++	++
Peritubular myoid cells	0	0	0	0	0	0	+
Vessel wall muscles	0	0	0	0	0	+	++

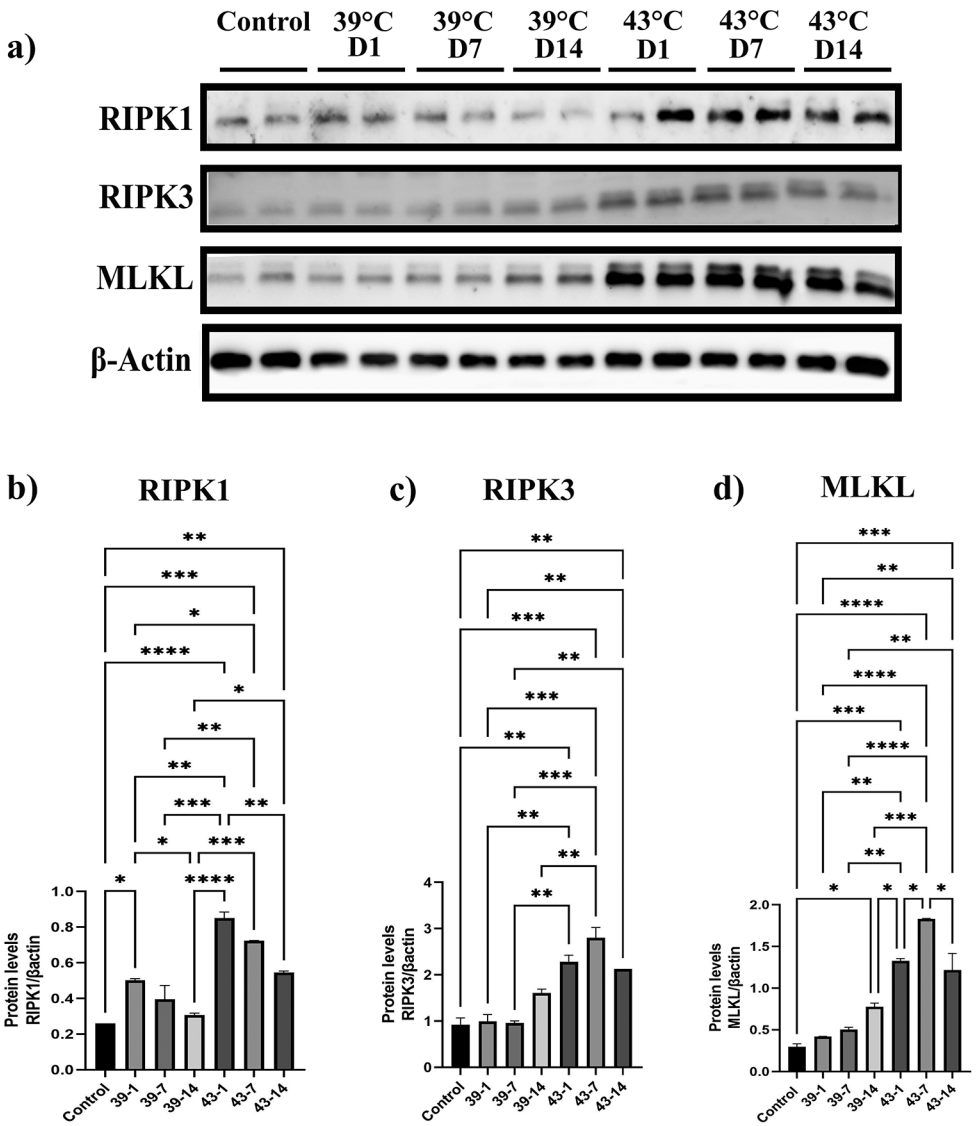

Fig. 6 Immunoblotting analysis of RIPK1, RIPK3 and MLKL. Band images of primary antibodies from all groups (**a**). Statistical graphic representation of the RIPK1/β actin protein ratio (**b**), RIPK3/β actin protein ratio (**c**), MLKL/β actin protein ratio (**d**). (*$p<0.05$, **$p<0.01$, ***$p<0.001$, ****$p<0.0001$)

group were observed on the 7th and 14th days ($p>0.05$) (Fig. 6a and b).

The RIPK1 protein level in the 43 °C heat stress group was higher than in the control group on the 1st and 7th days ($p<0.0001$ and $p<0.001$, respectively), (Fig. 6a and b). The RIPK1 protein level in the 43 °C heat stress group was higher than that in the control group on the 14th day ($p<0.01$), and also decreased compared to the 1st and 7th days ($p<0.01$ and $p<0.001$, respectively) (Fig. 6a and b).

No difference was determined in RIPK3 protein levels compared to the control group on the 1st, 7th, or 14th days of 39 °C heat stress ($p>0.05$) (Fig. 6a and b). The RIPK3 protein level increased on the 1st, 7th, and 14th days in the 43 °C heat stress group compared to the control group

($p<0.01$, $p<0.001$, and $p<0.01$, respectively) (Fig. 6a and c).

MLKL protein levels exhibited no difference compared to the control group on the 1st and 7th days of 39 °C heat stress ($p>0.05$), but rose relative to the control group on the 14th day ($p<0.05$) (Fig. 6a and d). No significant difference was observed between the groups' MLKL protein levels on the 1st day, 7th day and 14th days of 39 °C heat stress ($p>0.05$) (Fig. 6a and d).

When the results for the 1st, 7th, and 14th days of 43 °C heat stress were compared with the control group, an increase in MLKL protein levels was detected ($p<0.001$, $p<0.0001$, and $p<0.001$, respectively). However, the protein levels that increased on the 1st and 7th days exhibited a relative decreased on the 14th day ($p<0.05$) (Fig. 6a and d).

Discussion

Heat stress can interfere with spermatogenesis, leading to the death of germ cells and reduced fertility (Paul et al. 2009). In the present study, the presence of RIPK1, RIPK3 and MLKL, the main regulators of necroptosis, was detected in the testis tissues on the 1st, 7th, and 14th days following heat stress caused by different temperatures (39 °C and 43 °C) during a period of spermatogenesis. Their cellular localizations were detected immunohistochemically, and protein levels were determined quantitatively using the immunoblotting method. This study showed that heat stress caused by high temperature caused a loss of germ cells in the testis, with vacuoles being formed in germ cells and being shed from the seminiferous epithelium.

The Johnsen score assessment method has been used in many studies to evaluate testicular histology. This quantitative histological grading method is reliable, easily accessible and simple to estimate male reproductive potential. Therefore, we used the criteria developed by Johnsen to evaluate the histopathology of rat testes affected by scrotal heat stress in our study. According to our findings, the preservation of normal testicular architecture in the control group emphasizes the stability of basal physiological conditions. In the 39 °C group, the absence of significant changes in Johnsen scores on days 1 and 7 indicates that this temperature does not immediately compromise the histological integrity of the testicular tissue. However, the significant decrease observed on day 14 suggests that prolonged exposure to mild hyperthermia may compromise spermatogenesis and cell integrity. On the other hand, the 43 °C group showed a rapid and severe histological response with significant decreases in Johnsen scores starting on day 1 and gradually worsening on days 7 and 14. These findings suggest that acute exposure to higher temperatures causes immediate and extensive damage to the testicular tissue through various mechanisms. The results highlight the critical threshold effect of temperature on testicular function and emphasize the importance of maintaining optimum testicular temperature to preserve male reproductive health.

In another study, it was found that chronic heat exposure at 37 °C and 40 °C for 5 weeks in mice disrupted the histological architecture of testicular tissue and had a significantly reduced Johnsen score compared to the control group (Thanh et al. 2020). In another study using a similar heat stress value to our study, it was stated that after 14 days of exposure to heat stress at 43 °C for 15 min in mice, the Johnsen score in the heat-stressed group showed a significant decrease compared to the control group (Jeremy et al. 2022).

The levels of all three proteins increased at 43 °C on the 1st, 7th, and 14th days compared to the control group, while at 39 °C, RIPK1 increased on the 1st day and MLKL increased on the 14th day relative to the control group.

Necroptosis is a newly described form of lytic cell death and regulated necrosis (Huang et al. 2020). In case of absolute or relative absence of caspase-8 involvement, RIPK1 generally binds to RIPK3 to produce the necrosome in necroptosis. It subsequently phosphorylates the downstream pseudokinase mixed lineage kinase domain-like protein (MLKL). Additionally, the RIPK1/RIPK3/MLKL axis has been proposed as essential for regulating cellular necroptosis (Huang et al. 2020).

Studies have shown that systemic heat stress changes testis tissue composition, activates the TNFR1-dependent necroptosis pathway, and results in testis cell loss (Cai et al. 2023). In contrast to the ZBP1-RIPK3 pathway in other organs, testicular necroptosis is largely dependent on the TNFR1-RIPK1-RIPK3 pathway (Park et al. 2021).

A similar study to the present research reported that increased temperature in the testis tissue in animals that swam in a 43 °C water bath for 20 min triggered necroptosis by increasing MLKL expression levels in different hyperthermia groups (Hasani et al. 2022). MLKL is a molecule that penetrates and crosses the cell membrane, finally resulting in cell death.

Another study found that TNFR1-RIPK1-dependent necroptosis resulted in germ cell death in the mouse testis on the 7th and 14th days of 39 °C heat stress (Cai et al. 2023).

The present study described necroptosis-related signaling events in heat-induced cell death in testis tissues. Western blot and IHC analysis revealed a noteworthy rise in the protein expression levels of cell death markers at 39 °C and 43 °C compared with the control group. A one-degree rise in the temperature required for spermatogenesis causes a 14% decrease in spermatogenesis, and the atrophy of the

testes and impairment of spermatogenesis caused by heat stress causes male infertility. A distinguishing feature of the present study compared to others reporting necroptosis in heat stress is that the main regulators of heat stress were analyzed separately using immunohistochemical methods in the components of the testis tissue. In addition, two distinct temperature values (39 °C and 43 °C) were employed, and changes occurring on the 1st, 7th and 14th days of these applications were determined.

In addition to impairing sperm production and testicular structure, it has also been reported that necroptosis in the testes encourages aging-associated impairment of the male reproductive system in mice (Li et al. 2017).

Another study reported that RIPK1/RIPK3-dependent necroptosis caused by heat stress also occurs in pulmonary vascular endothelial cells (Huang et al. 2020) and intestinal epithelial cells (Zhou et al. 2023).

Research has also reported that heat stress adversely affects testicular structure and spermatogenesis, causing damage to germ cells, decreased sperm motility, and an increase in the proportion of sperm with abnormal morphology, testicular inflammation, and testicular interstitial fibrosis (Kanter et al. 2013; Nguyen-Thanh et al. 2022).

Heat stress aggravates testicular inflammation by activating and upregulating pro-inflammatory cytokines (tumor necrosis factor-alpha and interleukin 1 beta). This leads to spermatogenesis, infertility, and reduced sperm quality (Beigi Harchegani et al. 2020). The inflammatory response that occurs due to germ cell destruction in response to heat stress, tissue regeneration, and the signaling pathways involved in cell death following testicular hyperthermia, which affects the therapeutic strategy, need to be explained through molecular studies.

In addition, a previous study showed that heat stress compromises spermatogenesis by activating various non-apoptotic signaling pathways (pyroptosis, autophagy, and ferroptosis) and necroptosis in testicular tissue (Hasani et al. 2022). Further research into these death pathways will thus help develop therapeutic strategies against heat stress.

Conclusion

Our findings indicate an increase in necroptosis regulators, one of the non-apoptotic death pathways, in testis tissues at temperatures of 39 °C and 43 °C. The role of necroptosis in testicular damage due to increased temperature should, therefore, also be considered when evaluating therapeutic options.

Author contributions Musa TATAR: Conceptualisation, methodology, experiments performance, data obtain, supervision, funding acquisition, project administration. Kıymet Kübra TÜFEKCI: Data curation, formal analysis, statistical analysis, manuscript writing. Sema USLU: Data curation, formal analysis, statistical analysis, manuscript writing.

Funding This study was supported by the Scientific Research Foundation of Kastamonu University KÜBAP-01/2022-37.

Data availability No datasets were generated or analysed during the current study.

Declarations

Ethical approval The study protocol was approved by the Kastamonu University Experimental Animal Ethics Committee (date/number 24.06.2022/11), and conducted in accordance with the guide for the care and use of laboratory animals.

Competing interests The authors declare no competing interests.

References

Beigi Harchegani A, Dahan H, Tahmasbpour E, Bakhtiari Kaboutaraki H, Shahriary A (2020) Effects of zinc deficiency on impaired spermatogenesis and male infertility: the role of oxidative stress, inflammation and apoptosis. Hum Fertil (Camb) 23(1):5–16. https://doi.org/10.1080/14647273.2018.1494390

Boni R (2019) Heat stress, a serious threat to reproductive function in animals and humans. Mol Reprod Dev 86(10):1307–1323. https://doi.org/10.1002/mrd.23123

Cai H, Qin D, Liu Y, Guo X, Liu Y, Ma B, Hua J, Peng S (2023) Remodeling of gut microbiota by Probiotics Alleviated Heat Stroke-Induced necroptosis in male germ cells. Mol Nutr Food Res 67(18):e2300291. https://doi.org/10.1002/mnfr.202300291

Gu S, Huang C, Bai L, Chu C, Liu Q (2016) Heat-related illness in China, summer of 2013. Int J Biometeorol 60(1):131–137. https://doi.org/10.1007/s00484-015-1011-0

Hansen PJ (2009) Effects of heat stress on mammalian reproduction. Philos Trans R Soc Lond B Biol Sci 364(1534):3341–3350. https://doi.org/10.1098/rstb.2009.0131

Hasani A, Khosravi A, Rahimi K, Afshar A, Fadaei-Fathabadi F, Raoofi A, Raee P, Aghajanpour F, Aliaghaei A, Abdi S (2020) Photobiomodulation restores spermatogenesis in the transient scrotal hyperthermia-induced mice. Life Sci 254:117767

Hasani A, Khosravi A, Behnam P, Ramezani F, Eslami Farsani B, Aliaghaei A, Pirani M, Akaberi-Nasrabadi S, Abdi S, Abdollahifar MA (2022) Non-apoptotic cell death such as pyroptosis, autophagy, necroptosis and ferroptosis acts as partners to induce testicular cell death after scrotal hyperthermia in mice. Andrologia 54(2):e14320. https://doi.org/10.1111/and.14320

Huang W, Xie W, Gong J, Wang W, Cai S, Huang Q, Chen Z, Liu Y (2020) Heat stress induces RIP1/RIP3-dependent necroptosis through the MAPK, NF-kappaB, and c-Jun signaling pathways in pulmonary vascular endothelial cells. Biochem Biophys Res Commun 528(1):206–212. https://doi.org/10.1016/j.bbrc.2020.04.150

Hughes IA, Acerini CL (2008) Factors controlling testis descent. Eur J Endocrinol 159(Suppl 1):75–82. https://doi.org/10.1530/EJE-08-0458

Jeremy M, Gurusubramanian G, Kharwar RK, Roy VK (2022) Evaluation of a single dose of intra-testicular insulin treatment in heat-stressed mice model. Andrologia 54(11), e14603

Jiang Y, Liu Q, Zhao Y, Wang C, Sun M (2023) Activation of CREB-BDNF pathway in pyramidal neurons in the Hippocampus improves the neurological outcome of mice with ischemic stroke.

Mol Neurobiol 60(4):1766–1781. https://doi.org/10.1007/s12035-022-03174-x
Johnsen SG (1970) Testicular biopsy score count–a method for registration of spermatogenesis in human testes: normal values and results in 335 hypogonadal males. Hormones 1(1):2–25. https://doi.org/10.1159/000178170
Kanter M, Aktas C, Erboga M (2013) Heat stress decreases testicular germ cell proliferation and increases apoptosis in short term: an immunohistochemical and ultrastructural study. Toxicol Ind Health 29(2):99–113. https://doi.org/10.1177/0748233711425082
Kumar Roy V, Marak TR, Gurusubramanian G (2016) Alleviating effect of Mallotus roxburghianus in heat-induced testicular dysfunction in Wistar rats. Pharm Biol 54(5):905–918
Kurien BT, Scofield RH (2015) Western blotting: an introduction. Methods Mol Biol 1312:17–30. https://doi.org/10.1007/978-1-4939-2694-7_5
Li D, Meng L, Xu T, Su Y, Liu X, Zhang Z, Wang X (2017) RIPK1-RIPK3-MLKL-dependent necrosis promotes the aging of mouse male reproductive system. Elife 6. https://doi.org/10.7554/eLife.27692
Li L, Tan H, Zou Z, Gong J, Zhou J, Peng N, Su L, Maegele M, Cai D, Gu Z (2020) Preventing necroptosis by scavenging ROS production alleviates heat stress-induced intestinal injury. Int J Hyperth 37(1):517–530. https://doi.org/10.1080/02656736.2020.1763483
Meng MB, Wang HH, Cui YL, Wu ZQ, Shi YY, Zaorsky NG, Deng L, Yuan ZY, Lu Y, Wang P (2016) Necroptosis in tumorigenesis, activation of anti-tumor immunity, and cancer therapy. Oncotarget 7(35):57391–57413. https://doi.org/10.18632/oncotarget.10548
Morrell JM (2020) Heat stress and bull fertility. Theriogenology 153:62–67. https://doi.org/10.1016/j.theriogenology.2020.05.014
Murphy JM, Czabotar PE, Hildebrand JM, Lucet IS, Zhang JG, Alvarez-Diaz S, Lewis R, Lalaoui N, Metcalf D, Webb AI, Young SN, Varghese LN, Tannahill GM, Hatchell EC, Majewski IJ, Okamoto T, Dobson RC, Hilton DJ, Babon JJ, Nicola NA, Strasser A, Silke J, Alexander WS (2013) The pseudokinase MLKL mediates necroptosis via a molecular switch mechanism. Immunity 39(3):443–453. https://doi.org/10.1016/j.immuni.2013.06.018
Ngoula F, Lontio FA, Tchoffo H, Manfo Tsague FP, Djeunang RM, Vemo BN, Moffo F, Djuissi Motchewo N (2020) Heat induces oxidative stress: Reproductive Organ weights and serum Metabolite Profile, Testes structure, and Function Impairment in Male Cavy (Cavia porcellus). Front Vet Sci 7:37. https://doi.org/10.3389/fvets.2020.00037
Nguyen-Thanh T, Dang-Van P, Dang-Ngoc P, Kim W, Le-Minh T, Nguyen-Vu QH (2022) Chronic scrotal heat stress causes testicular interstitial inflammation and fibrosis: an experimental study in mice. Int J Reprod Biomed 20(7):569–580. https://doi.org/10.18502/ijrm.v20i7.11559
Park HH, Kim HR, Park SY, Hwang SM, Hong SM, Park S, Kang HC, Morgan MJ, Cha JH, Lee D, Roe JS, Kim YS (2021) RIPK3 activation induces TRIM28 derepression in cancer cells and enhances the anti-tumor microenvironment. Mol Cancer 20(1):107. https://doi.org/10.1186/s12943-021-01399-3
Paul C, Teng S, Saunders PT (2009) A single, mild, transient scrotal heat stress causes hypoxia and oxidative stress in mouse testes, which induces germ cell death. Biol Reprod 80(5):913–919. https://doi.org/10.1095/biolreprod.108.071779
Pryor RR, Roth RN, Suyama J, Hostler D (2015) Exertional heat illness: emerging concepts and advances in prehospital care. Prehosp Disaster Med 30(3):297–305. https://doi.org/10.1017/S1049023X15004628
Robinson N, McComb S, Mulligan R, Dudani R, Krishnan L, Sad S (2012) Type I interferon induces necroptosis in macrophages during infection with Salmonella enterica serovar typhimurium. Nat Immunol 13(10):954–962. https://doi.org/10.1038/ni.2397
Shakeel M, Yoon M (2023) Heat stress and stallion fertility. J Anim Sci Technol 65(4):683–697. https://doi.org/10.5187/jast.2023.e29
Skandhan KP, Rajahariprasad A (2007) The process of spermatogenesis liberates significant heat and the scrotum has a role in body thermoregulation. Med Hypotheses 68(2):303–307. https://doi.org/10.1016/j.mehy.2006.06.058
Thanh TN, Van PD, Cong TD, Le Minh T, Vu QHN (2020) Assessment of testis histopathological changes and spermatogenesis in male mice exposed to chronic scrotal heat stress. J Anim Behav Biometeorol 8(3):174–180
Wallach D, Kang TB, Dillon CP, Green DR (2016) Programmed necrosis in inflammation: toward identification of the effector molecules. Science 352(6281):aaf2154. https://doi.org/10.1126/science.aaf2154
Wang Y, Bobb JF, Papi B, Wang Y, Kosheleva A, Di Q, Schwartz JD, Dominici F (2016) Heat stroke admissions during heat waves in 1,916 US counties for the period from 1999 to 2010 and their effect modifiers. Environ Health 15(1):83. https://doi.org/10.1186/s12940-016-0167-3
Weinlich R, Oberst A, Beere HM, Green DR (2017) Necroptosis in development, inflammation and disease. Nat Rev Mol Cell Biol 18(2):127–136. https://doi.org/10.1038/nrm.2016.149
Wu J, Huang Z, Ren J, Zhang Z, He P, Li Y, Ma J, Chen W, Zhang Y, Zhou X, Yang Z, Wu SQ, Chen L, Han J (2013) Mlkl knockout mice demonstrate the indispensable role of Mlkl in necroptosis. Cell Res 23(8):994–1006. https://doi.org/10.1038/cr.2013.91
Xie Y, Chen H, Luo D, Yang X, Yao J, Zhang C, Lv L, Guo Z, Deng C, Li Y, Liang X, Deng C, Sun X, Liu G (2020) Inhibiting necroptosis of Spermatogonial Stem Cell as a Novel Strategy for male fertility preservation. Stem Cells Dev 29(8):475–487. https://doi.org/10.1089/scd.2019.0220
Xu H, Du X, Liu G, Huang S, Du W, Zou S, Tang D, Fan C, Xie Y, Wei Y, Tian Y, Fu X (2019) The pseudokinase MLKL regulates hepatic insulin sensitivity independently of inflammation. Mol Metab 23:14–23. https://doi.org/10.1016/j.molmet.2019.02.003
Zhou J, Qin X, Li L, Tian D, Zou Z, Gu Z, Su L (2023) Heat stress-induced intestinal epithelial cells necroptosis via TLR3-TRIF-RIP3 pathway was dependent on p53. Int Immunopharmacol 122:110574. https://doi.org/10.1016/j.intimp.2023.110574